Magnetic-field-enhanced outgoing excitonic resonance in multi-phonon Raman scattering from polar semiconductors

1996 J. Phys.: Condens. Matter 8 6769

(http://iopscience.iop.org/0953-8984/8/36/027)

J. Phys.: Condens. Matter **8** (1996) 6769–6778. Printed in the UK

Magnetic-field-enhanced outgoing excitonic resonance in multi-phonon Raman scattering from polar semiconductors

I G Lang†, A V Prokhorov†, M Cardona‡, V I Belitsky§, A Cantarero§ and S T Pavlov§‖

† A F Ioffe Physico-Technical Institute, Russian Academy of Sciences, 194021 St Petersburg, Russia

‡ Max Planck Institut für Festkörperforschung, Heisenbergstrasse 1, D-70569 Stuttgart, Germany

§ Departamento de Física Aplicada, Universidad de Valencia, Burjasot, E-46100 Valencia, Spain

Received 13 March 1996

Abstract. A combined scattering mechanism involving the states of free electron–hole pairs (exciton continuum) and discrete excitons as intermediate states in the multi-phonon Raman scattering leads to (i) a strong increase of the scattering efficiency in the presence of a high magnetic field and to (ii) an outgoing excitonic resonance. The two features are not compatible when only uncorrelated pairs (leading only to a strong increase of the scattering efficiency under the applied magnetic field) or discrete excitons (resulting in the outgoing resonance at the excitonic gap) are taken into account.

1. Introduction

In a recent publication [1], we have shown that the strong outgoing resonance observed in high-order multi-phonon resonant Raman scattering (MPRRS) from polar semiconductors can be explained when the high energy intermediate electronic states belong to the excitonic continuum (approximated by free electron–hole pairs, EHPs) and only couple to the bound excitonic state at the last stage of a scattering process. The high probability of decay into the continuum reduces the role of the MPRRS mechanism involving discrete excitons as the only intermediate states for explanation of the observed outgoing resonance at the ground excitonic transition (see [1] and references therein). Cooled by the emission of a sufficiently large number of LO phonons, the EHP binds into an exciton whose energy is not enough for LO-phonon-assisted decay.

In this work we analyse the effects of a high magnetic field on the outgoing excitonic resonance considering, as in [1], the monomolecular creation of a cold exciton by the light-generated free EHPs which lose energy but preserve their spatial correlation through the interaction with LO phonons.

2. Model

The main contribution to the Nth order MPRRS efficiency follows from processes with one (figure 1(a)) and two (figure 1(b)) bound excitonic intermediate states at the last stage of the elementary scattering process. Only these contributions correspond to the cascade

‖ On leave from the P N Lebedev Physical Institute, Russian Academy of Sciences, Moscow, Russia.

0953-8984/96/366769+10$19.50

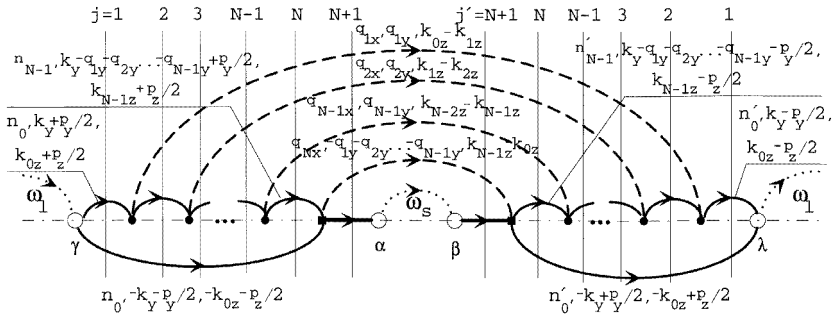

(*a*)

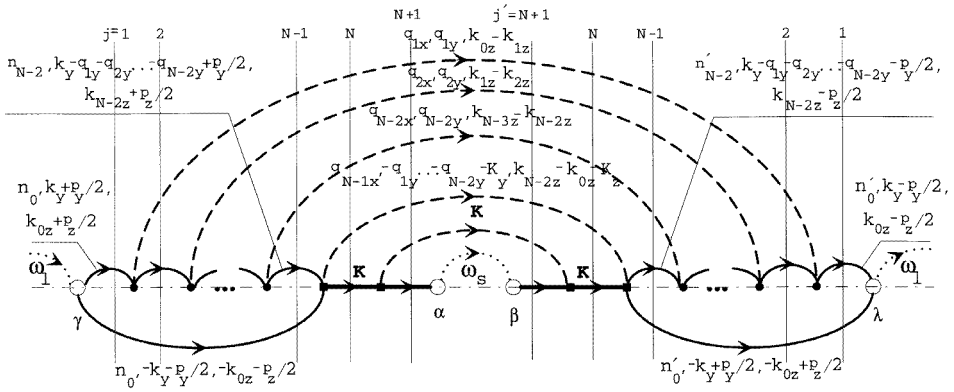

(*b*)

Figure 1. Two diagrams involving (*a*) one and (*b*) two discrete exciton intermediate states contributing to the MPRRS efficiency in the range of outgoing resonance. Hollow circles represent photon–EHP interaction and bold circles correspond to the electron–LO-phonon interaction while the square vertices are shown for transitions between two states of discrete exciton and for discrete–continuum transitions. Solid lines above (below) the dash–dotted line represent the electrons (holes) and horizontal lines bound excitons. Bold dashed lines connecting left- and right-hand sides of the diagrams correspond to LO phonons while the dotted lines represent the incident (on the left and right sides) and scattered (in the centre) photons.

of transitions where the bound exciton cannot decay into the EHP continuum through the emission of LO phonons. We assume $m_h \gg m_e$ so that the hole energy is less than the energy of one LO phonon and all phonons emitted by the EHP before its binding into a discrete exciton are emitted exclusively by the electron.

We use the Landau gauge $\boldsymbol{A} = \boldsymbol{A}(0, xH, 0)$ for a magnetic field directed along the z-axis and the corresponding wave functions of free EHPs. Only the ground state of the bound exciton is taken into account for discrete excitonic intermediate states in the last stage of the process. According to [2] and [3], the bound exciton wave function in a high magnetic field ($a \gg a_H$, where a is the Bohr radius in a zero magnetic field and a_H is the magnetic length, $a_H = \sqrt{hc/eH}$) can be written as

$$\Psi^{exc}_{\boldsymbol{K}_\perp K_z} = \Psi_{\perp \boldsymbol{K}_\perp} \Psi_{\parallel K_z}$$

where

$$\Psi_{\perp \boldsymbol{K}_\perp} = \frac{\exp\left[-|\boldsymbol{r}_\perp - \boldsymbol{r}_\perp(\boldsymbol{K}_\perp)|^2/(4a_H^2)\right]}{a_H\sqrt{2\pi L_x L_y}} \times \exp\left\{\mathrm{i}\left[(K_x - (y/a_H^2))R_x + K_y R_y + \Phi(\boldsymbol{r}_\perp, -\boldsymbol{K}_\perp) + C(K_x, K_y)\right]\right\} \tag{1}$$

and

$$\begin{aligned}\Phi(\boldsymbol{r}_\perp, -\boldsymbol{K}_\perp) &= \left(xy/a_H^2 - K_x x - K_y y\right)(m_e - m_h)/2M \\ C(K_x, K_y) &= a_H^2 K_x K_y (m_e - m_h)/2M\end{aligned} \tag{2}$$

m_e (m_h) is the electron (hole) effective mass, $M = m_e + m_h$, $\boldsymbol{r}_\perp(\boldsymbol{K}_\perp) = (a_H^2/H)[\boldsymbol{H} \times \boldsymbol{K}_\perp]$ and $\boldsymbol{R}$, $\boldsymbol{r}$ are the centre of mass and relative motion coordinates of an electron and hole. The longitudinal part $\Psi_{\parallel K_z}$ of the exciton wave function can be written as

$$\Psi_{\parallel K_z} = \frac{1}{\zeta\sqrt{a_\parallel L_z}} \exp(\mathrm{i}K_z R_z)\xi(z/a_\parallel) \tag{3}$$

where $\xi(s)$ describes the relative motion of the electron and hole along the magnetic field direction and satisfies the equation $\xi(s = 0) = 1$. The constant ζ is determined by the normalization condition

$$\zeta^2 = \int_{-\infty}^{\infty} \mathrm{d}s\ \xi^2(s).$$

We do not specify the exact form of $\xi(s)$ (see [2]) and introduce the two functions

$$\Theta(\alpha) = \int_{-\infty}^{+\infty} \mathrm{d}s \exp(\mathrm{i}\alpha s)\xi(s) \qquad \text{and} \qquad \eta(\alpha) = \int_{-\infty}^{+\infty} \mathrm{d}s \exp(\mathrm{i}\alpha s)\xi^2(s)$$

to be used below. For $\xi(s) = \exp(-|s|)$ one finds $\zeta = 1$, $\eta(\alpha) = 1/(1 + \alpha^2/4)$ and $\Theta(\alpha) = 2/(1+\alpha^2)$. The wave function of (1) reduces to that of [2] when the Landau gauge is changed for the symmetric one.

3. Scattering efficiency

The scattering efficiency can be written as [4]

$$\frac{\mathrm{d}^2 S}{\mathrm{d}\Omega \mathrm{d}\omega_s} = \frac{\omega_s^3 \omega_l}{c^4}\frac{n_s}{n_l} e^*_{s\alpha} e_{s\beta} e_{l\gamma} e^*_{l\lambda} S_{\alpha\gamma\beta\lambda}(\omega_l, \omega_s, \boldsymbol{\kappa}_l, \boldsymbol{\kappa}_s) \tag{4}$$

where $S_{\alpha\gamma\beta\lambda}$ is the light scattering tensor of rank four, c the light velocity in vacuum and n_l (n_s), $\mathbf{e}_l$ ($\mathbf{e}_s$), κ_l (κ_s) and u_l (u_s) are the refractive index, polarization vector, wave vector and group velocity of the incident (scattered) light, respectively. Using diagrammatic techniques, similar to those of [1], [3] and [5], we find for the contributions of the diagrams in figure 1(a) (figure 1(b))

$$\frac{\mathrm{d}^2 S_{Na(b)}}{\mathrm{d}\Omega \mathrm{d}\omega_s} = \sigma_0 \frac{\omega_s n_s}{\omega_l n_l} \frac{|\boldsymbol{e}_l \boldsymbol{p}_{cv}|^2 |\boldsymbol{e}_s \boldsymbol{p}_{cv}|^2}{\pi a_H^2 m_0^2 \hbar^2} \frac{\delta(\omega_l - \omega_s - N\omega_{LO})}{(\omega_s - \omega_{1H})^2 + (\gamma_{excH}(0)/2)^2} \frac{1}{L_{Na(b)}} \tag{5}$$

where $\sigma_0 = (e^2/m_0 c^2)^2$ and $\gamma_{excH}(0)$ is the inverse lifetime (broadening) of the exciton at the ground state with energy $E_{1H} = \hbar\omega_{1H}$. According to the assumption $m_h \gg m_e$, the

energy and the broadening of the hole have been neglected in all energy denominators. The quantity $L_{Na(b)}$ has dimensions of length and, for the diagram in figure 1(a)

$$\frac{1}{L_{Na}} = \sum_{\beta} \frac{D_{N\beta}}{\Lambda_{N\beta} Y_{N\beta}} \Xi_{n_0, n_{N-1}} \tag{6}$$

where the index β designates the sequence of transitions made by the electron through Landau bands emitting successively $N-1$ phonons. It represents the set of $n_0, n_1, \ldots, n_{N-1}$ Landau numbers and indices $i_1, i_2, \ldots, i_{N-1}$. Each index i may be 0 or 1: it is zero when the electron does not change the direction of motion along the magnetic field after the phonon emission and one when the sign of the velocity is opposite in the states before and after the phonon emission. In (6), $D_{N\beta}$ represents the integral

$$D_{N\beta} = \frac{1}{K_0 l} \int_0^{\infty} \prod_{j=1}^{N-1} \left[\frac{\mathrm{d}x_j}{K_j l} B_{n_{j-1} n_j}(x_j) \chi^{i_j}(K_{j-1}, K_j, x_j) \right] \left\langle B_{n_{N-1} n_0}(x_N) \chi^{i_N}(K_{N-1}, K_0, x_N) \right\rangle \tag{7}$$

where

$$K_j = +\sqrt{2m_e \left(\omega_l - \omega_{gH} - n_j \omega_{eH} - j\omega_{LO}\right)/\hbar} \qquad l = \sqrt{\hbar/(2m_e \omega_{LO})} \tag{8}$$

$$B_{nn'}(x) = \frac{\min(n!, n'!)}{\max(n!, n'!)} \mathrm{e}^{-x} x^{|n-n'|} \left[L^{|n-n'|}_{min(n,n')}(x) \right]^2 \tag{9}$$

and

$$\chi^i(K, K', x) = \left[x + a_H^2 (K \mp K')^2/2 \right]^{-1} \tag{10}$$

$\hbar\omega_{gH} = E_g + \hbar eH/(2\mu c)$, where $\mu = m_e m_h/M$ and E_g is the gap. In (10), the $-$ $(+)$ sign corresponds to $i = 0$ ($i = 1$).

Note that $i_N = 0$ when the direction of motion along the magnetic field after emission of $N-1$ phonons coincides with an initial direction. In this case, $s = \sum_{n=1}^{N-1} i_n$ is an even number. For odd s the direction of motion is opposite and $i_N = 1$. The symbol $\langle \ldots \rangle$ corresponds to the average over the directions of the wavevectors $\boldsymbol{q}_{1\perp}, \boldsymbol{q}_{2\perp}, \ldots, \boldsymbol{q}_{N-1\perp}$ in the xy-plane, when $x_j = a_H^2 q_{j\perp}^2/2$ and $\boldsymbol{q}_{N\perp} = -\sum_{i=1}^{N-1} \boldsymbol{q}_{i\perp}$. We used also

$$Y_{N\beta} = \prod_{j=0}^{N-1} (2\gamma_j/\alpha\omega_{LO}) \qquad \gamma_j = \gamma_e(n_j, K_j) \tag{11}$$

where α is the Fröhlich coupling constant. When $\gamma_e(n, |k_z|)$ is determined by the interaction with LO phonons, we find

$$\gamma_e(n, |k_z|) = \alpha\omega_{LO} \sum_{n'} (2l|k_z'|)^{-1} \int_0^{\infty} \mathrm{d}x B_{nn'}(x) \left[\chi^0(|k_z|, |k_z'|, x) + \chi^1(|k_z|, |k_z'|, x) \right]$$

$$k_z' = \sqrt{k_z^2 + 2m_e \left[\omega_{eH}(n-n') - \omega_{LO}\right]/\hbar}. \tag{12}$$

The sum over n' is limited by the condition that k_z' has to be real. When all $\gamma_0, \gamma_1, \ldots, \gamma_{N-1}$ are determined by the probability of emitting an LO phonon in a real transition, the substitution of (12) into (11) and multiplication of the result by l^N leads to $Y_{N\beta}$ defined in (134) of [5]. However, close to the resonance $\omega_s = \omega_{1H}$, the electron (after emitting $(N-1)$ LO phonons) occupies a state with energy less than the energy of an LO phonon. In this case γ_{N-1} is determined by some other weaker scattering mechanism:

$$\gamma_{N-1} = \Gamma_{N-1} \qquad \Gamma_{N-1} \ll \gamma_j \qquad j = 0, 1, \ldots, N-2. \tag{13}$$

This leads to the result

$$Y_{N\beta} = Y_{N-1\beta}\frac{2\Gamma_{N-1}}{\alpha\omega_{LO}}. \tag{14}$$

The length $\Lambda_{N\beta}$ is defined as

$$\Lambda_{N\beta} = f_{N\beta}^{-1}(z=0) \qquad f_{N\beta}(z) = f^{i_1 i_2 \ldots i_{N-1}}(z). \tag{15}$$

For example, in the case $N = 4$

$$f^{010}(z) = \left[f^{++--}(z) + f^{--++}(z)\right]/2$$

$$f^{++--}(z) = \frac{1}{\lambda_3}\int_{-\infty}^{\infty}\left[\prod_{j=0}^{j=2}\frac{\mathrm{d}z_j}{\lambda_j}\right]\Upsilon^{+}\left(\frac{z_0}{\lambda_0}\right)\Upsilon^{+}\left(\frac{z_1-z_0}{\lambda_1}\right)\Upsilon^{-}\left(\frac{z_2-z_1}{\lambda_2}\right)\Upsilon^{-}\left(\frac{z-z_2}{\lambda_3}\right) \tag{16}$$

$$\Upsilon^{+}(t) = \begin{cases} \mathrm{e}^{-t} & t > 0 \\ 0 & t < 0 \end{cases} \qquad \Upsilon^{-}(t) = \begin{cases} 0 & t > 0 \\ \mathrm{e}^{t} & t < 0 \end{cases} \tag{17}$$

$\lambda_j = \hbar K_j/m_e\gamma_j$ and $\gamma_j = \gamma_e(n_j, K_j)$.

In p-representation $f^{++--}(z)$ can be written as

$$f^{++--}(z) = \frac{1}{2\pi}\int_{-\infty}^{\infty}\frac{\mathrm{d}p\exp(\mathrm{i}pz)}{(1+\mathrm{i}\lambda_0 p)(1+\mathrm{i}\lambda_1 p)(1-\mathrm{i}\lambda_2 p)(1-\mathrm{i}\lambda_3 p)}. \tag{18}$$

Finally, we have used the definition

$$\begin{aligned}\Xi_{n_0,n_{N-1}} = \frac{1}{\zeta^4}[&\delta_{n_0,0}\Theta^2(a_\parallel K_0) + \delta_{n_{N-1},0}\Theta^2(a_\parallel K_{N-1}) \\ &- 2\delta_{n_0,0}\delta_{n_{N-1},0}\Theta(a_\parallel K_0)\Theta(a_\parallel K_{N-1})]\end{aligned} \tag{19}$$

where $\Theta(\alpha)$ has been defined after (3).

We proceed to calculate the contribution of the diagram in figure 1(b). Since one of the intermediate states for the process of figure 1(b) corresponds to an exciton with $\boldsymbol{K} \neq 0$, we need to comment on some details of the ground exciton dispersion $E_{exc}(K_\perp, |K_z|)$. The energy $E_{exc}(K_\perp, |K_z|)$ can be written as

$$E_{exc}(K_\perp, |K_z|) = E_{gH} + E(K_\perp) + \hbar^2 K_z^2/(2M). \tag{20}$$

The function $E(K_\perp)$ in some limits can be found in [2]. For our purposes it suffices to note that $E(K_\perp = 0) = -\Delta E_{1H}$ is the exciton binding energy in a high magnetic field and $E_{1H} = \hbar\omega_{1H} = E_{gH} - \Delta E_{1H}$. The contribution of the diagram in figure 1(b) is given by (5), where

$$\begin{aligned}\frac{1}{L_{Nb}} = \alpha\omega_{LO}\frac{M}{m_e}\int_0^{x_{max}}\mathrm{d}x\exp(-x)&\frac{[\eta(a_\parallel K_{z0}m_h/M) - \eta(a_\parallel K_{z0}m_e/M)]^2}{\zeta^4\left(x + a_H^2K_{z0}^2/2\right)^2 l K_{z0}\gamma_{exc}(x, K_{z0})} \\ &\times\sum_\beta\frac{R_{N-1\beta}(x, K_{z0})}{\Lambda_{N-1\beta}Y_{N-1\beta}}.\end{aligned} \tag{21}$$

$K_{z0} = \sqrt{2M\left[\omega_l - \omega_{gH} - E(x)/\hbar - (N-1)\omega_{LO}\right]/\hbar}$ is the absolute value of the z-component of an exciton wave vector in the Nth real intermediate state, $x = a_H^2K_\perp^2/2$, and $\eta(\alpha)$ has been defined after (3). The $K_{\perp max}$ is a maximum value of $K_\perp$ allowed by energy conservation, i.e., under the condition that K_{z0} is real. At variation of $K_\perp$ from zero to infinity the value $E(x)$ changes from $-\Delta E_{1H}$ to zero [6]. Therefore, in the range $\omega_l > \omega_{gH} + (N-1)\omega_{LO}$, we have $x_{max} \to \infty$, whereas for $\omega_{1H} + (N-1)\omega_{LO} <$

$\omega_l < \omega_{gH} + (N-1)\omega_{LO}$ the values of $K_{\perp max}$ and x_{max} are determined by the equation $\hbar\omega_l - E_{gH} - (N-1)\hbar\omega_{LO} = E(K_{\perp max})$. We used also the following definitions:

$$R_{N-1\beta}(K_\perp, K_{z0}) = \frac{1}{lK_0}\int_0^\infty \prod_{j=1}^{N-2}\left[\frac{\mathrm{d}x_j}{lK_j} B_{n_{j-1}n_j}(x_j)\chi^{i_j}(K_{j-1}, K_j, x_j)\right] \times \left\langle B_{n_{N-2}n_0}(x_{N-1}) P_\beta(K_\perp, K_{z0})\right\rangle \tag{22}$$

$$P_\beta(K_\perp, K_{z0}) = \left[\Upsilon_\beta(K_\perp, K_{z0}) + \Upsilon_\beta(K_\perp, -K_{z0})\right]/2 \tag{23}$$

and

$$\begin{aligned}\Upsilon_\beta(K_\perp, K_{z0}) = \zeta^{-4}\Big\{ & x_{N-1} + (a_H^2/2)\left[(-1)^p K_{N-2} - K_0 - K_{z0}\right]^2\Big\}^{-1} \\ & \times\Big\{\delta_{n_0,0}\Theta^2\left[a_\parallel\left(K_0 + m_h K_{z0}/M\right)\right] + \delta_{n_{N-2},0}\Theta^2\left[a_\parallel\left((-1)^p K_{N-2} + m_e K_{z0}/M\right)\right] \\ & -2\delta_{n_0,0}\delta_{n_{N-2},0}\Theta\left[a_\parallel\left(K_0 + \frac{m_h}{M}K_{z0}\right)\right]\Theta\left[a_\parallel\left((-1)^p K_{N-2} - \frac{m_e}{M}K_{z0}\right)\right] \\ & \times\cos\left[a_H^2\left(\boldsymbol{q}_{N-1}\times\boldsymbol{K}_\perp\right)\right]\Big\}\end{aligned} \tag{24}$$

where β is a set of indexes $n_0, n_1, \ldots, n_{N-2}, i_1, i_2, \ldots, i_{N-2}$, $p = \sum_{n=1}^{N-2} i_n$. The variables of integration in (22) are $x_j = a_H^2 q_{j\perp}^2/2$ with a constraint $\boldsymbol{q}_{N-1\perp} = -\sum_{i=1}^{N-2}\boldsymbol{q}_{i\perp} - \boldsymbol{K}_\perp$. The symbol $\langle\cdots\rangle$ denotes the average over angles which determine the direction of vectors $\boldsymbol{q}_{1\perp}, \boldsymbol{q}_{2\perp}, \ldots, \boldsymbol{q}_{N-2\perp}, \boldsymbol{K}_\perp$ in the xy-plane.

4. Applicability limits

Let us discuss the applicability limits of the expressions for contributions of diagrams in figure 1. We assume that $\Delta E_{1H} < \hbar\omega_{LO}$ and consider four intervals for the laser frequency:

(i) $\omega_{1H} + (N-1)\omega_{LO} < \omega_l < \omega_{gH} + (N-1)\omega_{LO}$

(ii) $\omega_{gH} + (N-1)\omega_{LO} < \omega_l < \omega_{1H} + N\omega_{LO}$

(iii) $\omega_{1H} + N\omega_{LO} < \omega_l < \omega_{gH} + N\omega_{LO}$

(iv) $\omega_l > \omega_{gH} + N\omega_{LO}$. (25)

The frequency width of the intervals (i) and (iii) is $\Delta E_{1H}/\hbar$ and that of interval (ii) is $(\omega_{LO} - \Delta E_{1H}/\hbar)$. The outgoing excitonic resonance coincides with the boundary of intervals (ii) and (iii).

Equations (5) and (6) for the contribution of the diagram in figure 1(a) are valid when K_{N-1} is real for $n_{N-1} = 0$ (see (8)). This is satisfied within the intervals (ii), (iii) and (iv). In intervals (ii) and (iii), the value of $K_N(n_N = 0)$ is pure imaginary and it is real in interval (iv). This means that γ_{N-1} is determined by (13) in (ii) and (iii) (therefore, in the vicinity of the outgoing resonance) and (14) is valid. Let us show that the Γ_{N-1} cancels out of the expression for the contribution of the diagram in figure 1(a). To do this note that $\Lambda_{N\beta}$ from (15) is proportional to the mean free path

$$\mathcal{L}_{N-1} = \frac{\hbar K_{N-1}}{m_e\Gamma_{N-1}} \tag{26}$$

when $\mathcal{L}_{N-1} \gg \lambda_j$, $j = 0, 1, \ldots, N-2$. Thus,

$$\Lambda_{N\beta}^{-1} = \mathcal{L}_{N-1}^{-1} T_{N\beta} \tag{27}$$

where $T_{N\beta}$ is a dimensionless function of $\lambda_0, \lambda_1, \ldots, \lambda_{N-2}$. For $N = 2$ we find [3] that $(\Lambda_{20})^{-1} = f^0(z=0) = 0$, $(\Lambda_{21})^{-1} = f^1(z=0) = 1/(\lambda_0 + \lambda_1)$. This leads to

$T_{20} = 0$, $T_{21} = 1$. Likewise, for $N = 3$, $(\Lambda_{300})^{-1} = f^{00}(z = 0) = 0$, $(\Lambda_{310})^{-1} = f^{10}(z = 0) = \lambda_0/((\lambda_0 + \lambda_1)(\lambda_0 + \lambda_2))$, $(\Lambda_{311})^{-1} = f^{11}(z = 0) = \lambda_1/((\lambda_1 + \lambda_0)(\lambda_1 + \lambda_2))$, $(\Lambda_{301})^{-1} = f^{01}(z = 0) = \lambda_2/((\lambda_2 + \lambda_0)(\lambda_2 + \lambda_1))$. For $\lambda_2 \to \mathcal{L}_2$ this leads to $T_{300} = 0$, $T_{310} = \lambda_0/(\lambda_0+\lambda_1)$, $T_{311} = \lambda_1/(\lambda_0+\lambda_1)$ and $T_{301} = 1$. Using (14), (27) and (26) we obtain

$$\left(Y_{N\beta}\Lambda_{N\beta}\right)^{-1} = (Y_{N-1\beta})^{-1}\frac{\alpha\omega_{LO}m_e}{2\overline{h}K_{N-1}}T_{N\beta}. \tag{28}$$

Thus, the quantity Γ_{N-1} does not appear in the final result.

Equations (5) and (21) for the contribution of figure 1(b) are valid when K_{z0} is real which is true for all four frequency intervals. In (ii), (iii) and (iv) the broadening γ_{N-2} is determined by the probability of emitting an LO phonon, while $\gamma_{N-2} \to \Gamma_{N-2}$ in (i), where $\Gamma_{N-2} \ll \gamma_j$, $j = 0, 1, \ldots, N-3$. Note that (21) does not contain Γ_{N-2} in the interval (i) as it was shown above. The contribution of figure 1(b) depends strongly on the behaviour of $\gamma_{exc}(K_\perp, K_{z0})$ in the denominator of (21). This is the inverse relaxation time of the exciton in the state with energy $E_{exc}(K_\perp, K_{z0}) = \overline{h}\omega_l - (N-1)\overline{h}\omega_{LO}$. For $E_{exc}(K_\perp, K_{z0}) > E_{1H} + \overline{h}\omega_{LO}$ the value of $\gamma_{exc}(K_\perp, K_{z0})$ is determined by the probability of emitting an LO phonon and is proportional to α. However, for $E_{exc}(K_\perp, K_{z0}) < E_{1H} + \overline{h}\omega_{LO}$, the real emission of one LO phonon is impossible and $\gamma_{exc}(K_\perp, K_{z0})$ is determined by other much weaker processes, so that $\gamma_{exc}(K_\perp, K_{z0}) \to \Gamma_{exc}(K_\perp, K_{z0})$, with $\Gamma_{exc} \ll \gamma_{exc}$. The change of the scattering mechanism dominating the broadening takes place at the frequency corresponding to the outgoing excitonic resonance. Below this point, the contribution of figure 1(b) exceeds strongly that of figure 1(a). Note that in this range we have to take into account other contributions involving processes with acoustic phonons (see below).

Finally, the pole approximation (i.e., real transitions) for integrals over $k_{0z}, k_{1z}, \ldots, k_{N-1z}$ for the contribution of figure 1(a) and over $k_{0z}, k_{1z}, \ldots, k_{N-2z}$ for figure 1(b) results in the constraints $N \geqslant 2$ and $N \geqslant 3$ for (6) and (21), respectively.

Strongly out of the resonance, a two-band model is not a good approximation. To reproduce the observed overall factor $\omega_s^3\omega_l$ in the scattering efficiency one needs to sum over a large number of intermediate states. In this case it is better to use another expression for the transition matrix element [8] which is equivalent to the one we use but gives better convergence and displays the $\omega_s^3\omega_l$ factor in any order of summation.

5. Discussion and conclusions

Let us consider the resonant behavior of the MPRRS efficiency as a function of H and ω_l. We limit ourselves to the case $N \geqslant 3$ where both (6) and (21) are valid. Both contributions increase in the vicinity of $K_0 = 0$, which corresponds to $\omega_{lmax,m_h\to\infty} \simeq \omega_{gH} + n\omega_{eH}$. Taking into account the finite value of m_h leads to an exact relation $\omega_{lmax}(n) = \omega_{gH} + eHn/\mu c$. This condition corresponds to the creation of EHPs in the vicinity of the Landau band bottoms. The resonant conditions can be achieved by changing either H or ω_l. The maxima in a magnetic field dependence take place at

$$H_{max}(n) = \frac{\mu c}{e}\frac{\omega_l - \omega_g}{n + 1/2} \tag{29}$$

being independent of the order N of the scattering process. For $N = 3$ there is an additional resonance [3] corresponding to the contribution of figure 1(b) at $\omega'_{lmax,m_h\to\infty} \simeq \omega_{gH} + neH/m_e c + \omega_{LO}$. This resonance follows from the increase of $(\Lambda_{21})^{-1} = 1/(\lambda_0+\lambda_1) = 1/(\overline{h}K_0/m_e\gamma_0 + \overline{h}K_1/m_e\gamma_1)$ in (21), when $K_1 \to 0$, because of the divergence in γ_0 (see (12)). Note also that the contribution of figure 1(b) is equal to zero [3] for $\omega_{lmin,m_h\to\infty}(n, N-1) = \omega_{gH} + neH/m_e c + (N-1)\omega_{LO}$.

Above the outgoing resonance the contributions of figure 1(*a*) and figure 1(*b*) in the MPRRS efficiency are of the same order of magnitude. However, as mentioned before, below the resonance the contribution of figure 1(*b*) strongly increases because of the strong increase in the exciton lifetime in the real intermediate state with the energy being too small for emission of an LO phonon. In this range, other scattering processes such as the absorption of LO phonons, interaction with acoustic phonons, etc have to be taken into account. We give now a qualitative picture of the process including in our consideration the distribution function of excitons with respect to $K_\perp$, $|K_z|$. Let us introduce the integral efficiency for the Nth order process as

$$S_N = \int\int \frac{\mathrm{d}^2 S_N}{\mathrm{d}\Omega\,\mathrm{d}\omega_s}\mathrm{d}\Omega\,\mathrm{d}\omega_s = \frac{1}{u_l}\sum_{\kappa_s}\bar{W}_{sN} \tag{30}$$

where u_l is the group velocity of incident light and $\bar{W}_{sN}$ the normalized probability of emitting the scattered light quantum per unit time [7]. Equation (30) differs from (5) only by the absence of the factor $4\pi\delta(\omega_l - \omega_s - N\omega_{LO})$.

On the other hand,

$$\sum_{\kappa_s}\bar{W}_{sN} = \sum_{K_\perp, K_z} P_{excN-1}(K_\perp, |K_z|)\gamma_l(K_\perp, |K_z|) \tag{31}$$

where $P_{excN-1}(K_\perp, |K_z|)$ is the normalized dimensionless distribution function of excitons created by the light in an $N-1$ LO-phonon-assisted process and $\gamma_l(K_\perp, |K_z|)$ the probability of an LO-phonon-assisted emission of the scattered light quantum which can be written as $\gamma_l(K_\perp, |K_z|) = \sum_{\kappa_s} w_s$ and

$$w_s = \frac{2\pi}{\hbar}\sum_f \left|\sum_a \frac{\langle f|U_s|a\rangle\langle a|\mathcal{H}_{int}|i\rangle}{E_i - E_a + \mathrm{i}\hbar\gamma_a/2}\right|^2 \delta(E_i - E_f) \tag{32}$$

$\mathcal{H}_{int}$ is the Fröhlich interaction of the exciton with LO phonons and U_s represents the interaction of excitons with the light. The initial and final state energy are $E_i = E_{exc}(K_\perp, |K_z|)$ and $E_f = \hbar\omega_s + \hbar\omega_{LO}$, respectively. The intermediate state energy $E_a = E_{aEHP} + \hbar\omega_{LO}$ includes both the discrete and continuum part of the excitonic dispersion. Let us separate γ_l into two corresponding parts, $\gamma_l = \gamma_{ldisc} + \gamma_{lcont}$. The outgoing resonance is related to the contribution γ_{ldisc0} to γ_{ldisc} from the transition via the ground state of the exciton. According to (32), we find

$$\gamma_{ldisc0}(K_\perp, |K_z|) = 4\frac{n_s\omega_s}{\hbar c^3}\left(\frac{e}{m_0}\right)^2 |\boldsymbol{e}_s\boldsymbol{p}_{cv}|^2 \frac{\alpha\omega_{LO}^2 l}{K_\perp^2 + K_z^2} \times \frac{\exp\left(-a_H^2 K_\perp^2/2\right)}{a_\parallel a_H^2 \zeta^6} \frac{[\eta(K_z a_\parallel m_h/M) - \eta(K_z a_\parallel m_e/M)]^2}{[\omega_{exc}(K_\perp, |K_z|) - \omega_{1H} - \omega_{LO}]^2 + \gamma_{excH}^2(0)/4}. \tag{33}$$

Above the excitonic resonance, $\omega_l > \omega_{1H} + N\omega_{LO}$, we have

$$P_{excN-1}(K_\perp, |K_z|) = \frac{W_{excN-1}(K_\perp, |K_z|)}{\gamma_{exc}(K_\perp, |K_z|)} \tag{34}$$

where $W_{excN-1}(K_\perp, |K_z|)$ is the normalized number of excitons created per unit time in the volume V_0 in the $(N-1)$-LO-phonon-assisted process. The probability $W_{excN-1}(K_\perp, |K_z|)$ has been calculated in [3] for $N = 4$. When used in (34) together with (33), (30) and (31) it reproduces the result of (5) and (21).

Note that above the outgoing resonance the distribution is not zero only in a very narrow interval of energies [3] since $W_{excN-1}(K_\perp, |K_z|)$ is proportional to $\delta[\omega_l - (N-1)\omega_{LO} -$

$E_{exc}(K_\perp, |K_z|)/\hbar$]. However, for ω_l below the resonance the distribution becomes smooth. If the most important mechanism in this range is the interaction with acoustic phonons, one has to take into account diagrams with external acoustic phonon lines. In the range (ii) (see (25)) the smoothing of the distribution should be weaker than in the range (i). The reason for this is the kinetic energy of excitons in range (ii) which is larger than the exciton binding energy. Since the probabilities of scattering and decay via the interaction with phonons are of the same order, the exciton decays after a few interactions with acoustic phonons. The decay of an exciton in range (i) is suppressed because of its small energy. In this case, the distribution depends on the probability of non-radiative recombination. At zero magnetic field, the distribution of excitons in range (i) has been considered in [9]–[12].

The smoothness of the distribution leads to (a) the broadening of the MPRRS peaks in the range (ii) and especially in the range (i) and to (b) the increase of the integrated scattering intensity, since the diagrams with acoustic phonon lines give additional contributions to the MPRRS efficiency.

To summarize, we have shown that the outgoing excitonic resonance becomes strongly enhanced under a high magnetic field. Above the outgoing resonance, the scattering efficiency for $N \geqslant 3$ may be up to α^{-2} times stronger than in a zero magnetic field where the MPRRS efficiency [1] is proportional to α^3, whereas in a high magnetic field it is proportional to α, as follows from (5), (6) and (21). The crossover from α^3 to α results from the quasi-one-dimensional character of free EHPs in N (figure 1(a)) or $N-1$ (figure 1(b)) intermediate states under a high magnetic field. The enhancement is also valid for the ranges (i) and (ii) below the excitonic resonance, where one has to calculate the exciton distribution function taking into account the interaction with acoustic phonons. To the best of our knowledge such calculations have yet to be performed. However, the distribution function is proportional to the creation probability of excitons with energy in the interval between zero and $\hbar\omega_{LO}$ which is increased by α^{-2} times in a high magnetic field [3]. Thus, the MPRRS efficiency also increases below the excitonic resonance.

The integrated efficiency as a function of ω_l has to be asymmetric with respect to the point $\hbar\omega_l = N\hbar\omega_{LO} + E_{1H}$ because of the strong increase in the exciton lifetime below the resonance and appearance of additional contributions from the processes with acoustic phonons.

Acknowledgments

VIB and STP thank the European Union, Ministerio de Educación y Ciencia de España (DGICYT) and the Russian Fundamental Investigation Fund (93-02-2362, 950204184A) for financial support and the University of Valencia for its hospitality. This work has been partially supported by grant PB93-0687 (DGICYT).

References

[1] Belitsky V I, Cantarero A, Pavlov S T, Cardona M, Prokhorov A V and Lang I G 1995 *Phys. Rev.* B **52** 11 920

[2] Gor'kov L P and Dzyaloshinsky I E 1967 *Zh. Eksp. Teor. Fiz.* **53** 717 (Engl. transl. 1968 *Sov. Phys.–JETP* **26** 449)

[3] Lang I G, Pavlov S T and Prokhorov A V 1994 *Zh. Eksp. Teor. Fiz.* **106** 244 (Engl. transl. 1994 *Sov. Phys.–JETP* **79** 133)

[4] Pavlov S T 1979 *Dr Sci Thesis* St Petersburg State University p 290
Ivchenko E L, Lang I G and Pavlov S T 1977 *Fiz. Tverd. Tela* **19** 1751 (Engl. transl. 1977 *Sov. Phys. Solid State* **19** 718)

Ivchenko E L, Lang I G and Pavlov S T 1978 *Phys. Stat. Solidi* b **85** 81
[5] Belitsky V I, Cardona M, Lang I G and Pavlov S T 1992 *Phys. Rev.* B **46** 15 767
[6] For $a_H^2 K_\perp^2 \simeq a^2/a_H^2$ there is no bound exciton in a high magnetic field ($a \ll a_H$). However, in the integral of (21) only the range $x \leqslant 1$ is important, a fact which allows us to integrate in the interval between zero and infinity.
[7] Lang I G, Pavlov S T, Prokaznikov A V and Goltsev A V 1985 *Phys. Stat. Solidi* b **127** 187
[8] Zeyher R, Bilz H and Cardona M 1976 *Solid State Commun.* **19** 57
[9] Gross E F, Permogorov S A and Travnikov V V J. 1970 *Phys. Chem. Solids* **31** 2595
[10] Planel R, Bonnot A and Benoit à la Guillaume C 1973 *Phys. Stat. Solidi* b **58** 251
[11] Trallero Giner C, Sotolongo Costa O, Lang I G and Pavlov S T 1986 *Fiz. Tverd. Tela* **28** 2075 (Engl. transl. 1986 *Sov. Phys. Solid State* **28** 1160)
[12] Trallero Giner C, Sotolongo Costa O, Lang I G and Pavlov S T 1986 *Fiz. Tverd. Tela* **28** 3152 (Engl. transl. 1986 *Sov. Phys. Solid State* **28** 1774)